Second International Conference on Coastal Zone Engineering and Management (Arabian Coast 2010), November 1-3, 2010, Muscat, Oman
ISSN: 2219-3596

Undular Bores

Hubert Chanson

School of Civil Engineering, The University of Queensland, Brisbane, Australia

Abstract: A tidal bore is a series of waves propagating upstream as the tidal flow turns to rising, forming during the spring tides when the tidal range exceeding 4 to 6 m is confined into a narrow funnelled estuary. The existence is based upon a fragile hydrodynamic balance between the tidal amplitude, the freshwater river flow conditions and the river channel bathymetry, and it is shown that this balance may be easily disturbed by changes in boundary conditions and freshwater inflow. The very large majority of tidal bore have an undular shape, with the leading wave followed by a train of well-developed undulations or whelps. The undular bore propagates upstream relatively slowly and the free-surface undulations have a smooth appearance; little wave breaking is observed but close to the banks or above sand banks. The meteorological equivalent is the undular bore cloud pattern observed in Northern Australia and over the Arabian Sea for example. Herein the basic hydrodynamics of undular bores is reviewed and presented using both field and laboratory data, and the analogy with the atmospheric bore is discussed.

Key words: Undular bores, Tidal bores, Morning Glory, Internal waves.

1. Introduction

A hydraulic jump is the rapid transition from a high-velocity open channel flow to a slower fluvial motion. It is a sharp discontinuity in terms of the water depth as well as the pressure and velocity fields (Lighthill 1978). A hydraulic jump in translation results from a sudden change in flow that increases the depth. Called a positive surge or bore, it is the quasi-steady flow analogy of the stationary hydraulic jump (Henderson 1966, Liggett 1994). In an estuary, a tidal bore is an unsteady flow motion generated by the rapid water level rise at the river mouth during the early flood tide. With time, the leading edge of the tidal wave becomes steeper and steeper until it forms a wall of water: i.e., the tidal bore that is a hydraulic jump in translation (Fig. 1a).

The flow properties immediately before and after the tidal bore must satisfy the continuity and momentum principles (Rayleigh 1908, Henderson 1966, Liggett 1994). The integral form of the equations of conservation of mass and momentum gives a series of relationships between the flow properties in front of and behind the bore front. For a horizontal channel and neglecting bed friction, it yields:

$$\frac{d_2}{d_1} = \frac{1}{2} \times \left(\sqrt{1 + 8 \times Fr_1^2} - 1 \right) \quad [1]$$

$$\frac{Fr_2}{Fr_1} = 2^{3/2} \Big/ \left(\sqrt{1 + 8 \times Fr_1^2} - 1 \right)^{3/2} \quad [2]$$

where:
d_1 = initial flow depth, m
d_2 = new flow depth, m
Fr_1 =tidal bore Froude number
Fr_2 = Froude number defined in terms of new flow conditions

The Froude number Fr_1 of the tidal bore is defined in the system of co-ordinates in translation with the bore front. For a rectangular channel, it is:

$$Fr_1 = \frac{V_1 + U}{\sqrt{g \times d_1}} \quad [3]$$

where:
V_1 = initial flow velocity positive downstream, m/s
U = tidal bore celerity positive upstream, m/s
g = gravity acceleration, m/s^2

The Froude number Fr_1 is always greater than unity. For $Fr_1 < 1$, the tidal wave cannot become a tidal bore. For $1 < Fr_1 < 1.5$ to 1.8, the tidal bore front is followed a train of well-formed, quasi-periodic undulations: i.e. the undular bore (Fig. 1a). For $Fr_1 > 1.5$ to 1.8, the bore front had a marked roller associated with some air entrainment and turbulent mixing: i.e., the breaking tidal bore (Chanson 2010).

A key feature of hydraulic jumps and tidal bores is the intense turbulent mixing generated by the bore propagation (Henderson 1966, Parker 1996, Koch and Chanson 2009). In a natural system, the formation and occurrence of bores have some major impact on the sediment processes (Macdonald et al. 2009), as well as on the ecology including fish egg dispersion (Rulifson and Tull 1999). Recently it was argued that the long-lasting impact of the

undulations has a major impact on the turbulence and water column mixing (Koch and Chanson 2008, Chanson and Tan 2011). A historical anecdote is the tidal bore of the Indus River that wiped out the fleet of Alexander the Great in BC 325 (Arrian 1976, Quintus Curcius 1984); the Indus River mouth is seen in Figure 1b (Top right).

(a) Undular tidal bore of the Dordogne River (France) on 27 September 2008 - The two kayakers were riding the second wave and the surfer was on the third wave

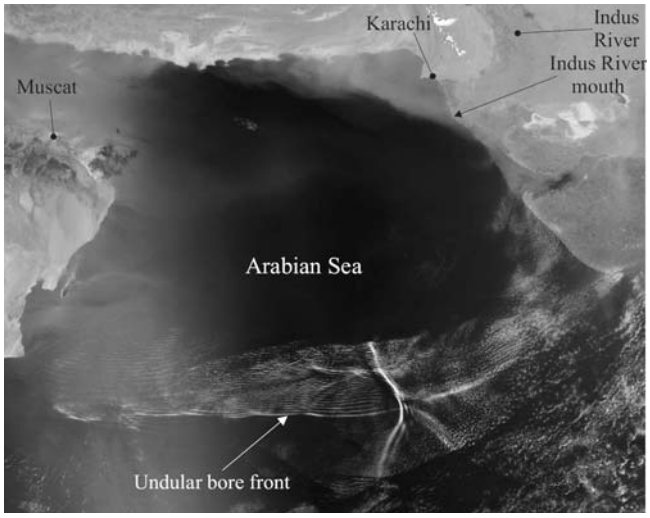

(b) Undular cloud formation (undular bore) over the Arabian Sea on 8 May 2007 (Courtesy of NASA Earth Observatory and Jeff SCHMALTZ, MODIS Rapid Response System at NASA GSFC)

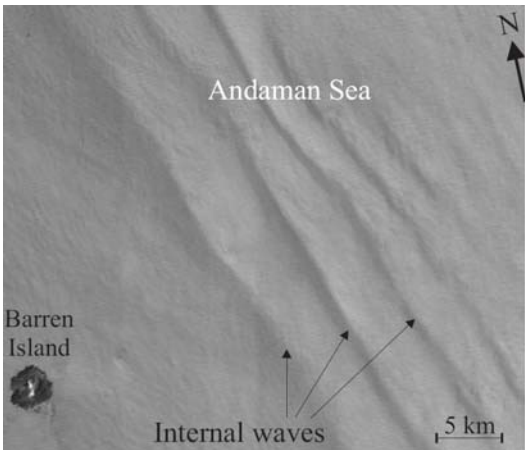

(c) Internal undular bore on the Indian Ocean near the Andaman Islands on 6 March 2007 (Courtesy of NASA Earth Observatory)

Figure 1. Undular bores

A related undular flow situation is the undular cloud formation sometimes called an undular jump or undular bore (Fig. 1b), observed in Northern Australia for example where it is called a "Morning Glory" (Clarke 1972, Clarke et al. 1981). The cloud formation is basically a large cluster of wave clouds spanning across hundreds of kilometres (Fig. 1b). The undular cloud formation is usually created by the interaction between some cool, dry air in a low-pressure system with a stable layer of warm, moist air. When the two air masses clash, the colder air pushes the warm air upwards. Some disturbances develop at the interface and the flow pattern has a similar appearance to an undular tidal bore. These undular bores are thought to be catalysts for thunderstorms. While a thunderstorm may assist with the occurrence of an undular bore, an undular bore can in turn intensify a thunderstorm because it further disturbs the atmosphere. Undular bores are thought also to have some adverse impact on the air traffic (Lillie 1978). There are several reports of severe incidents involving commercial aircrafts hit by turbulence when they encountered what is believed to be an undular bore, including an Airbus A319 above the Canadian Rocky Mountains on 10 January 2009.

Undular waves can occur at surfaces between different density layers within the ocean (Davis and Acrivos 1967, Wood and Simpson 1984, Dyer 1997). The deeper waters are cold, dense, and salty, while the shallower water layer is warmer, lighter and fresher. The differences in density and salinity cause these internal waves (Fig. 1c). The waves may be caused by strong vertical velocity gradients (e.g. strong tidal currents), non-linear transfer from surface waves, and inverted barometric effects including short-period variations in wind stress (Pond and Pickard 1991).

In this study, the basic features of undular tidal bores are reviewed and developed. The analogy and differences with atmospheric undular bores are discussed.

2. Undular Tidal Bores: Free-Surface Properties

Basic flow patterns

The physical observations (Table 1) highlight several flow patterns depending upon the tidal bore Froude number Fr_1. For $Fr_1 < 1.5$ to 1.8, the tidal bore is followed a train of well-formed undulations: i.e., an undular bore. The bore has a smooth two-dimensional profile for $Fr_1 < 1.25$ (Fig. 1a). For $1.25 < Fr_1$, some slight cross-waves or shock waves are observed, developing next to the sidewalls upstream of the first wave and intersecting next to the first wave crest. A similar cross-wave pattern is observed in stationary undular hydraulic jumps (Chanson and Montes 1995, Ben Meftah et al. 2007). For $1.3 < Fr_1 < 1.5$ to 1.8, some light breaking is observed at the first wave crest, and the free-surface undulations become flatter. The cross-waves are also observed.

For larger Froude numbers ($Fr_1 > 1.5$ to 1.8), the undulations disappear and the bore is characterised by a marked turbulent roller. Some air entrainment and turbulent mixing are observed in the roller. Behind the breaking bore front, the free-surface is basically two-dimensional.

For a wide range of physical investigations (Table 1), the basic flow patterns are consistent with the early findings of Bazin (1865) and others. Importantly the flow patterns are basically independent of the initial steady flow conditions.

Table 1. Physical investigations of tidal bores

Reference	V_1 m/s	d_1 m	Remarks
Favre (1935)	0	0.106 to 0.206	B = 0.42 m
Treske (1994)	--	0.08 to 0.16	B = 1 m
Koch & Chanson (2008)	1.0	0.079	B = 0.5 m
Chanson (2010)	0.83	0.14	B = 0.5 m. Smooth and rough beds.
Chanson (2011)	0.19 to 0.92	0.056 to 0.20	B = 0.5 m
Chanson & Tan (2011)	0.1 to 1	0.0505 to 0.196	B = 0.5 m
Field data Ponsy &Carbonell (1966)	--	--	Oraison intake channel (France)
Lewis (1972)	0 to 0.2	0.9 to 1.4	Dee River (UK) near Saltney Ferry
Navarre (1995)	0.65 to 0.7	1.12 to 1.15	Dordogne River (France) at St Pardon
Wolanski et al. (2004)	0.15	1.5 to 4	Daly River (Australia)

Undular free-surface profile

The key feature of an undular bore is the secondary wave pattern (Fig. 2). Figure 2 shows the dimensionless time-variations of the water depth at three longitudinal distances along a laboratory channel during the same experiment. In an undular bore, the equation of conservation of momentum may be applied across the jump front together with the equation of conservation of mass (Henderson 1966, Liggett 1994, Chanson 1999). When the rate of energy dissipation is negligible as in an undular tidal bore, there is a quasi-conservation of energy. Let us follow the tidal bore in the system of coordinates in translation with the undular bore front. The equations of conservation of momentum and energy may be rewritten as:

$$\frac{M}{d_c^2} = \frac{d_c}{d} + \frac{1}{2} \times \left(\frac{d}{d_c} \right)^2 = \text{constant} \quad [4]$$

$$\frac{E}{d_c} = \frac{d}{d_c} + \frac{1}{2} \times \left(\frac{d_c}{d} \right)^2 = \text{constant} \quad [5]$$

where:
M = momentum function, m
E = specific energy per unit mass, m
d = flow depth, m
d_c = critical flow depth, m

For a tidal bore, the critical flow depth d_c is:

$$d_c = \sqrt[3]{\frac{((V_1 + U) \times d_1)^2}{g}} \quad [6]$$

The equation of conservation of momentum [4] is applicable to any type of hydraulic jumps and bores. The equation of conservation of energy [5] is on the other hand an approximation that is valid only for small Froude numbers close to unity, like undular bores. In an undular bore, the equations [4] and [5] form a parametric representation of the relationship between the dimensionless momentum and specific energy (Benjamin and Lighthill 1954, Montes 1986). The relationship has two branches intersecting at the critical flow conditions ($d = d_c$) for $M/d_c^2 = 1.5$ and $E/d_c = 1.5$ (Fig. 3). The two branches represent the only possible relationship between the dimensionless momentum function and specific energy in an undular tidal bore as long as both equations [3] and [4] are valid. In Figure 3, the right branch corresponds to the supercritical flow and the upper branch is associated with the subcritical flow. Figure 4 illustrates a comparison between theory and physical data. The graph includes the initial flow conditions, the first wave crest and the undular flow data for the first three wave lengths. Note a seemingly greater momentum function and specific energy at the first wave crest than in the initial flow. This is linked with the assumption of hydrostatic pressure distributions in Equations [4] and [5]; in an undular bore, the streamline curvature implies a non-hydrostatic pressure field in the undular flow. Basically the pressure gradient is greater than

hydrostatic beneath wave troughs and less than hydrostatic under wave crests.

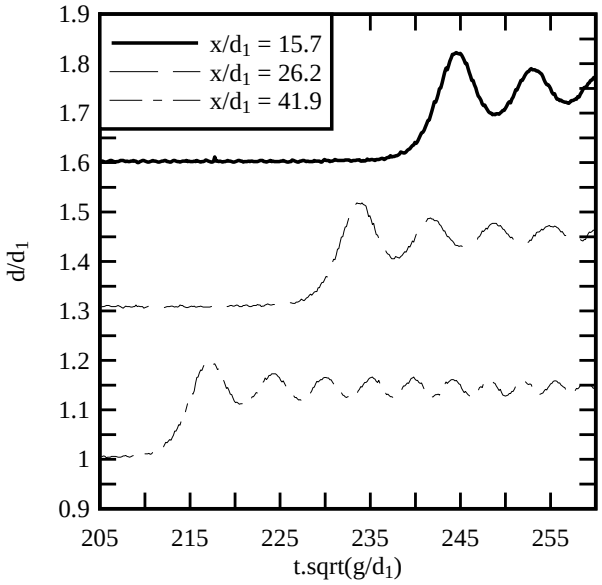

Figure 2. Dimensionless free-surface profiles during the propagation of an undular bore: d_1 = 0. 191 m, Fr_1 = 1.11, U = 1.32 m/s (Data: Chanson 2011) - Each curve is offset vertically by 0.3

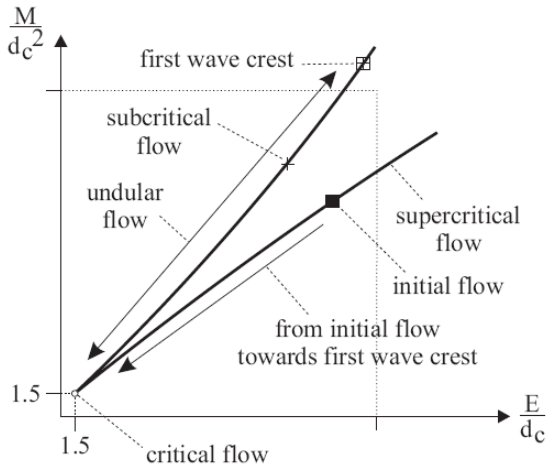

Figure 3. Definition sketch of the relationship between dimensionless momentum and specific energy in undular bores

The secondary wave motion presents a smooth undular shape (Fig. 1, 2, 5 & 6). Figures 5 and 6 show some field observations of undular bores, and the measurements are compared with the linear wave theory (sinusoidal curve) (Lemoine 1948) and Boussinesq equation solution (cnoidal wave function) (Benjamin and Lighthill 1954). Although the theoretical solutions are fitted between a crest (or trough) and the next trough (or crest) for each half-wave length, the agreement between the data and analytical solutions is disappointing. Neither theory can capture the fine details of the free-surface profile shape nor the asymmetrical wave shape (Chanson 2011). A comparison highlights the largest deviations between a wave crest and the next trough, with lesser differences between a wave trough and next crest (Fig. 5 & 6).

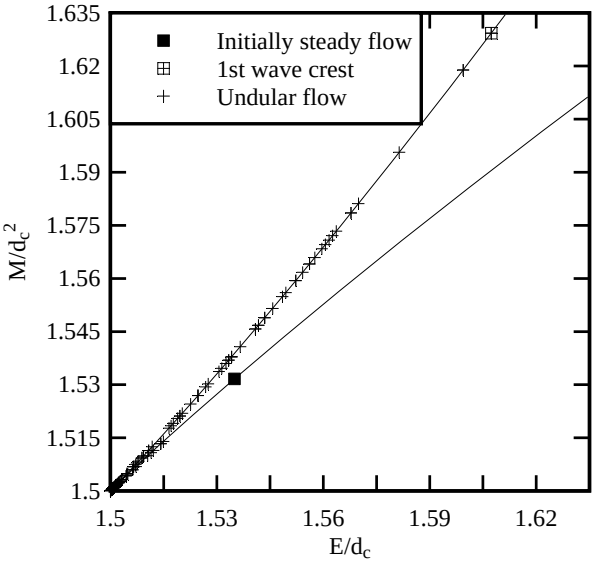

Figure 4. Dimensionless relationship between momentum function and specific energy in an undular tidal bore: d_1 = 0.0802 m, Fr_1 = 1.22, U = 0.862 m (Data: Chanson 2011)

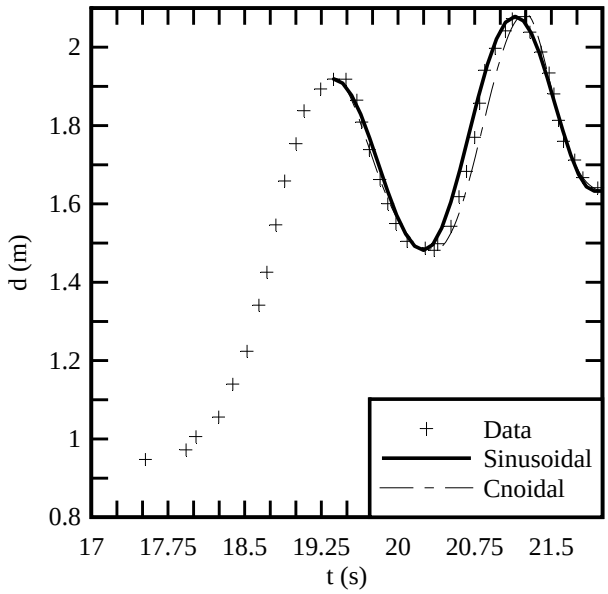

Figure 5. Free-surface profile of the Dee River undular tidal bore on 22 September 1972: d_1 = 0.941 m, Fr_1 = 1.5, U = 3.44 m/s (Data: Lewis 1972)

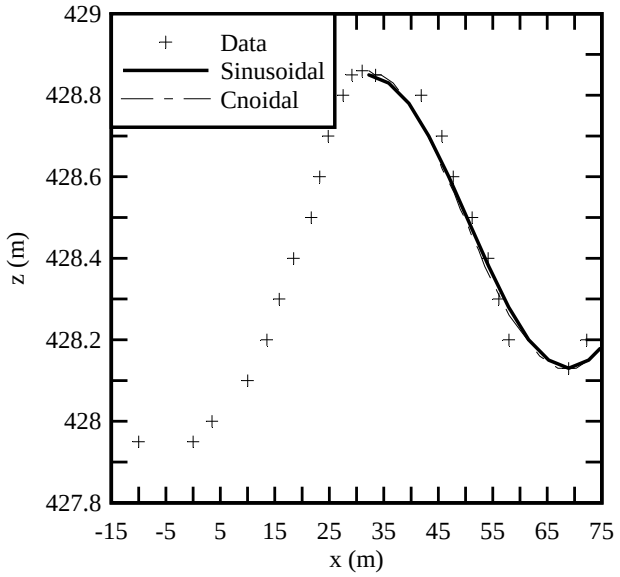

Figure 6. Free-surface profile of an undular bore in the Oraison intake channel: longitudinal variation of the water elevation, U = 5 to 6 m/s (Data: Ponsy and Carbonnell 1966)

Free-surface undulations characteristics

The water elevations on either side of the bore front must satisfy the equation of conservation of momentum (Eq. [1]). The ratio of the water depths d_2/d_1 is presented as a function of the bore Froude number in Figure 7 where Equation [1] is compared with some physical data. The comparison indicates some reasonable agreement, even if Equation [1] is developed neglecting boundary friction and assuming hydrostatic pressure distribution. Yet the result is consistent with a large number of observations (Henderson 1966, Montes 1998).

Some characteristics of the free-surface undulations are presented in Figure 8 and 9, showing respectively the dimensionless wave length L_w/d_1 and wave steepness a_w/L_w as functions of the Froude number for a range of initial flow depths (Table 1). L_w and a_w are respectively the length and amplitude of the first wave defined between the first and second wave crests. The wave length data indicate a decreasing wave length with increasing Froude number (Fig. 8). Both laboratory and field observations highlight that the wave steepness a_w/L_w increases with increasing Froude number for Froude numbers slightly greater than unity until a local maximum (Fig. 9). The maximum in wave steepness is linked with the apparition of some light wave breaking and energy dissipation at the first wave crest for $Fr_1 \sim 1.3$ to 1.4. The physical data shown in Figure 9 are compared to the analytical solutions of Lemoine (1948) and Andersen (1978) respectively based upon the linear wave theory and the Boussinesq equations. The physical data tend to follow more closely the linear wave theory solution (Lemoine 1948). While the Boussinesq equation is more accurate when the pressure distribution deviates from hydrostatic, the linear wave theory is simpler in engineering practice. It is noteworthy that the physical data indicate that the theoretical developments are applicable only for a narrow range of Froude numbers ($1 < Fr_1 < 1.3$ to 1.35).

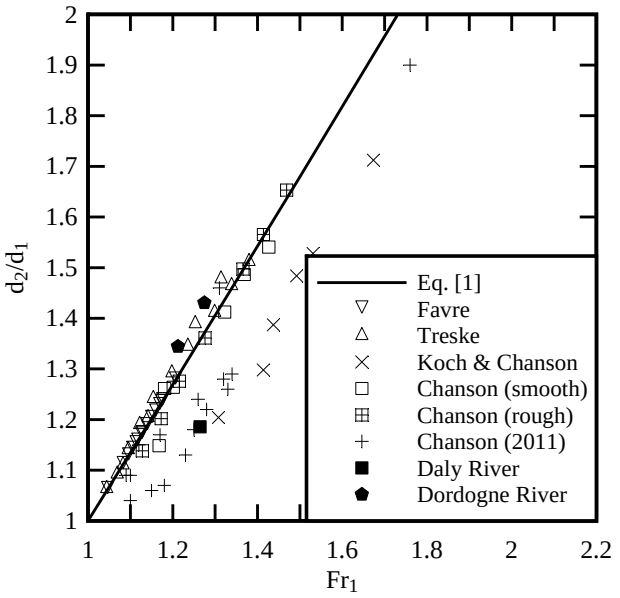

Figure 7. Ratio of conjugate depths d_2/d_1 in undular tidal bores

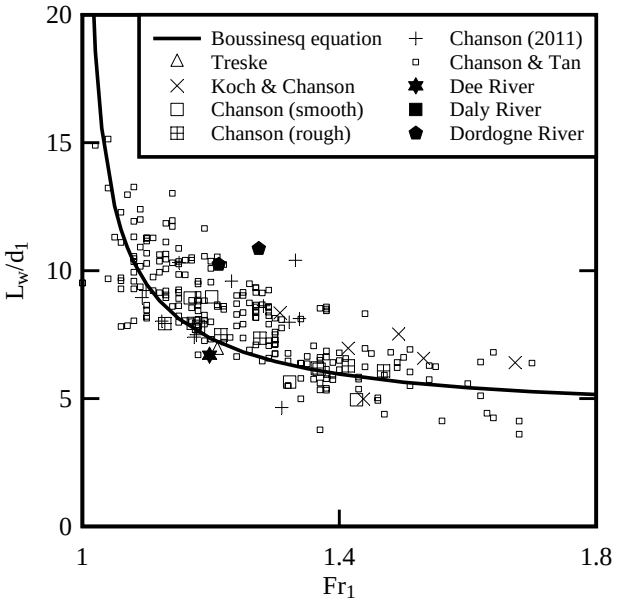

Figure 8. Dimensionless wave length L_w/d_1 in undular tidal bores

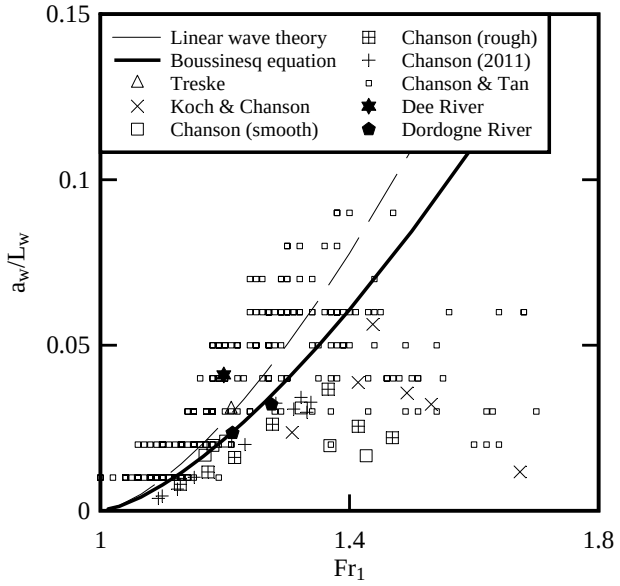

Figure 9. Dimensionless w ave s teepness a $_w/L_w$ in undular tidal bores

Wave energy

The total energy of the free-surface undulations is the sum of potential and kinetic energy. The potential energy may estimated simply from free-surface measurements and used as a proxy of the total energy.

Over a wave length, the potential energy equals the integral of the weight of water above the mean water level times the distance to the centroid:

$$\text{P.E.} = \int_0^{L_w} \frac{1}{2} \times \rho \times g \times \eta^2 \times B \times dx \qquad [7]$$

where:
η = water elevation relative to the mean water elevation over the wave length, m
B = channel width, m

Equation [7] is based upon the assumption of a two-dimensional wave motion (Liggett 1994). The water elevation η is estimated relative to the average water level over the wave length. Figure 10 illustrates the integration process. When the water level is recorded as a function of time at a fixed location, the potential energy over a wave period T can be obtained by a change of variables:

$$\text{P.E.} = \int_0^{T} \frac{1}{2} \times \rho \times g \times \eta^2 \times U \times B \times dt \qquad [8]$$

The potential energy per unit surface area equals:

$$E_p = \frac{\text{P.E.}}{U \times T \times B} = \frac{1}{T} \times \int_0^{T} \frac{1}{2} \times \rho \times g \times \eta^2 \times dt \qquad [9]$$

Some typical experimental data are presented in Figure 11, where the dimensionless potential energy per unit area is shown as a function of the dimensionless distance x/d_1. On the graph, the tidal generation takes place at $x/d_1 = 139$ and the bore propagates upstream (right to left in Fig. 11). The data show typically an increasing potential energy with increasing distance from the tidal bore generation location up to $x/d_1 = 75$. Further upstream, the tidal bore profile become invariant with distance, and the potential energy of the undulations are thereafter quasi-constant. The laboratory data highlight a greater potential energy per unit area in the first wave length than in the subsequent wave lengths as seen in Figure 11.

The potential energy of free-surface undulations may be compared with the total potential energy per surface area of the tidal bore itself:

$$(E_p)_{bore} = \frac{1}{T} \times \int_0^{T} \frac{1}{2} \times \rho \times g \times (d - d_1)^2 \times dt \qquad [10]$$

Some recent laboratory data indicate that the potential energy of undulations may represent up to 30% of the total potential energy of the undular tidal bore. Figure 12 illustrates some physical data, and the results suggest a decrease with increasing wave length number (Fig. 12). The largest ratio of potential energy of undulations to total potential energy of undular bore is recorded for $Fr_1 \sim 1.3$ corresponding to the apparition of light breaking at the first wave crest.

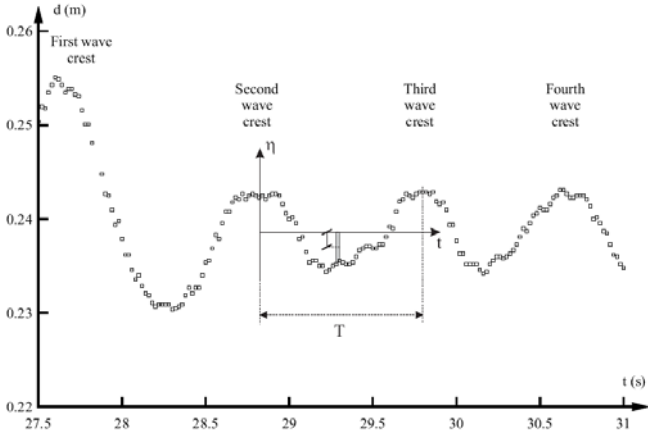

Figure 1 0. Potential energy i ntegration al ong a n undular bore wave length

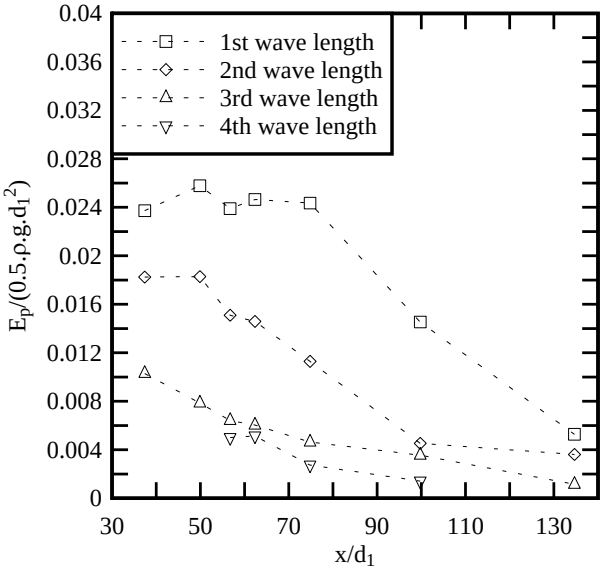

Figure 11. Di mensionless pote ntial ener gy per surface area in an un dular bore: d_1 = 0 .0802 m, Fr_1 = 1.22, U = 0.862 m/ s (D ata: Chanson 20 11) - B ore prop agation from right to left

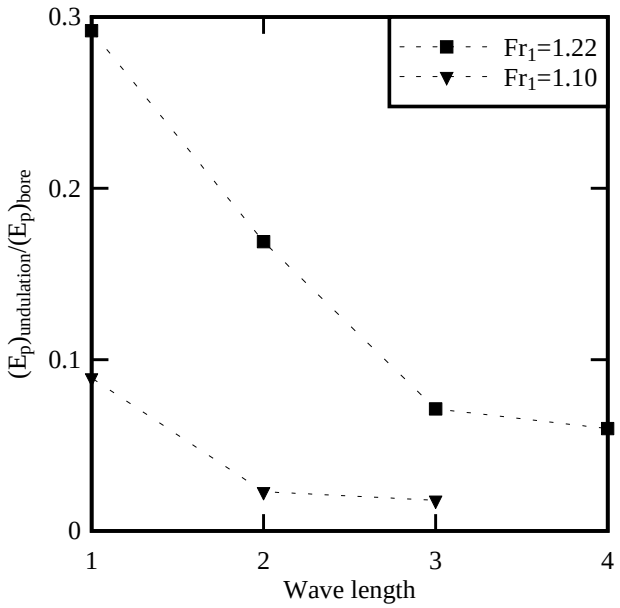

Figure 12. Rati o of pote ntial energy of free-s urface undulations to bore potential energy as a function of the wave length number: x/d_1 = 62.5 (Data: Chanson 2011)

3. Turbulent Mixing in Undular Tidal Bores

Both field and laboratory measurements show some large velocity fluctuations associated with intense turbulent mixing during the bore propagation (Hornung et al. 1995, Koch and Chanson 2008) (Table 1). Figure 13 illustrates some physical data of instantaneous velocity data in undular tidal bores.

The undular bore is characterised by a smooth wave crest followed by a series of free-surface undulations. When the undular bore front passes above the sampling volume of the velocity probe, a relatively gentle longitudinal deceleration is observed at all vertical elevations (Fig. 13). The longitudinal velocity component V_x is minimum beneath the wave crest and it oscillates with the same period as the surface undulations and out of phase. V_x is maximum beneath the wave troughs and minimum below the wave crests at all vertical elevations. Close to the free-surface, the vertical velocity V_z data present also an oscillating pattern (not shown in Figure 13). The basic flow net theory predicts these redistributions in longitudinal and vertical velocity components since the free-surface is a streamline (Rouse 1938, Chanson 2009) (Fig. 14). Further the instantaneous velocity data show some large fluctuations of all velocity fluctuations, including the transverse velocities V_y on the channel centreline (Fig. 13). The findings imply the existence of transient secondary currents behind the bore front. These intense turbulent events are observed at several longitudinal locations highlighting an upstream advection process.

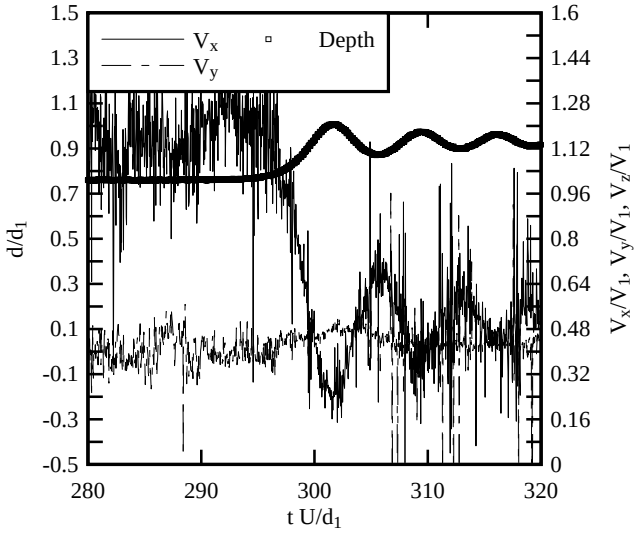

(a) On a smooth bed: d_1 = 0.199 m, Fr_1 = 1.08, U = 1.32 m/s, z/d_1 = 0.18 (Data: Chanson 2011)

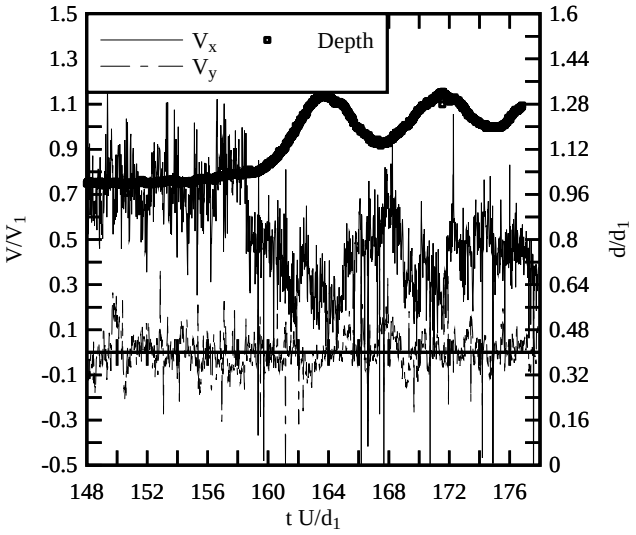

(b) On a rough bed: d_1 = 0.141 m, Fr_1 = 1.20, U = 0.551 m/s, z/d_1 = 0.18 (Data: Chanson 2010)

Figure 13. Dimensionless instantaneous turbulent velocity components in undular tidal bores

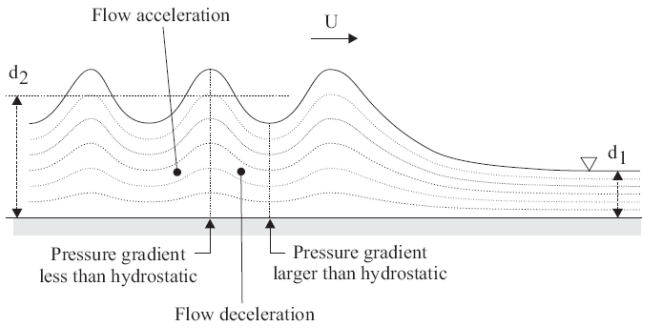

Figure 14. Streamline pattern in an undular tidal bore with an irrotational flow motion

The physical data are associated with some large fluctuating turbulent stresses below the bore front and beneath the whelps. The Reynolds stress levels are significantly larger than before the bore passage, and large normal and tangential stresses are observed (Fig. 15). The large Reynolds stresses recorded beneath the secondary waves suggest the long lasting sediment mixing beneath the "whelps" (Chanson 2005, Koch and Chanson 2008). A comparison between undular and breaking tidal bores show that (a) the magnitude of turbulent stresses is comparable, but (b) the large fluctuations in Reynolds stresses last for a significantly longer period beneath the undular bore. The finding implies that the undular tidal bores may contribute to significant bed scour in tidal bore affected estuaries.

The energetic turbulent events illustrated in Figures 13 and 15 are some form of "macro-turbulence", or large-scale turbulence, produced beneath the tidal bore front and advected upstream behind the tidal bore. The evidences of advected macro-turbulence behind a tidal bore are documented in the field: e.g., in the Mersey River (UK) and Rio Mearim (Brazil), in the Daly River (Australia) and the northern Branch of the Changjiang River estuary. Considering a tidal bore propagating upstream, it induces some intense turbulent mixing, and some strong turbulent kinetic energy production caused by secondary motion occurs beneath the undulations, as sketched in Figure 16. The turbulent events interact with the mean flow and some energetic "clouds" of turbulence are advected within the main flow behind the bore. The turbulent bursts are not only linked with the undular bores, but are observed also in breaking bores (Hornung et al. 1995, Koch and Chanson 2009). The turbulence "patches" are generated below the bore front and the vorticity production rate proportional to $(Fr_1-1)^3$. The vorticity "clouds" are a basic feature of tidal bores as shown by some recent numerical results (Furuyama and Chanson 2008, Lubin et al. 2010). In non-prismatic natural channels, the secondary current motion and macro-turbulence are further enhanced by the irregular bathymetry.

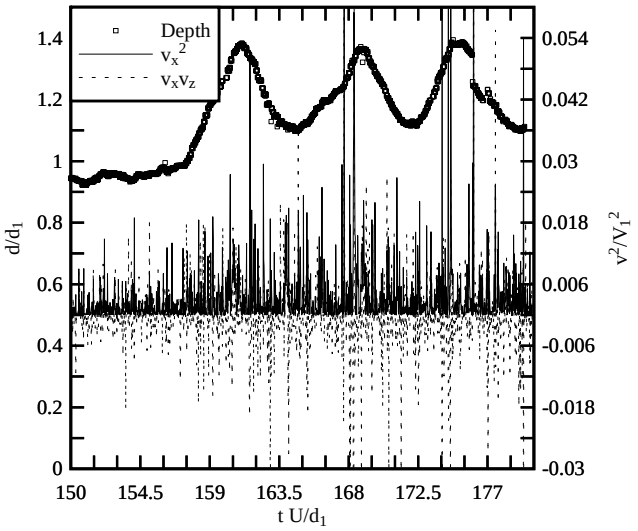

Figure 15. Dimensionless instantaneous turbulent stresses v_x^2/V_1^2 and $v_x v_z/V_1^2$ in an undular bore: d_1 = 0.138 m, Fr_1 = 1.17, U = 0.553 m/s, z/d_1 = 0.76 (Data: Chanson 2010)

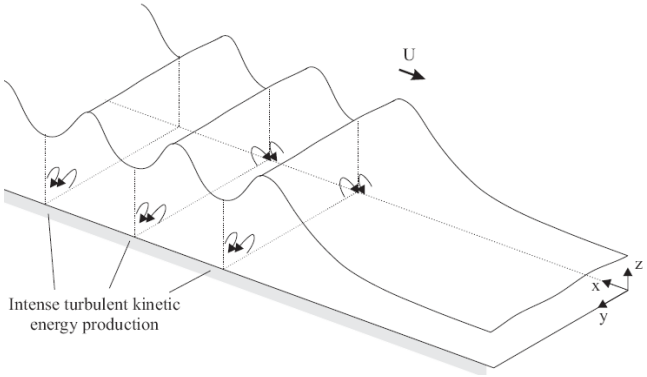

Figure 1 6. S econdary currents gener ated during a undular tidal bore propagation

4. Undular Bores in the Atmosphere

Some unusually long transitory/wave cloud formation may occur in the atmosphere when a denser air layer advances underneath a lighter layer. Figure 1b shows a large-scale example while Figure 17 illustrates a more local event. Figure 18 presents a two-dimensional schematic. In the atmosphere, the propagation speed of internal waves is:

$$C = \sqrt{g' \times d} \quad [11]$$

where:
d = dense layer thickness, m
g' = reduced gravity, m/s^2

$$g' = -g \times \Delta\rho / \rho \quad [12]$$

ρ = dense layer density, kg/m^3
$\Delta\rho$ = density difference cross the fluid interface, kg/m^3

Considering an undular bore in the atmosphere (Fig. 18), the Froude number is defined as:

$$Fr_1 = \frac{U}{C_1} = \frac{U}{\sqrt{g' \times d_1}} \quad [13]$$

where:
U = front propagation speed, m/s

In some variably stratified atmospheric conditions with wind shear, it may be difficult to define uniquely a Froude number. However a number of field observations showed some conditions with a sharp density interface associated with an atmospheric undular bore (Clarke et al. 1981, Doviak and Ge 1984, Burk and Haack 2000). The application of the momentum equation yields the classical result:

$$\frac{d_2}{d_1} = \frac{1}{2} \times \left(\sqrt{1 + 8 \times Fr_1^{\,2}} - 1 \right) \quad [1]$$

in which the undular bore Froude number is defined in terms of the specific gravity (Eq. [13]). A key feature of undular cloud formation is the size of the geophysical process. The field observations show some dense layer thickness and front celerity within: d_1 ~ 150 to 9,000 m and U ~ 6 to 15 m/s. The arrival of the undular bore is usually associated with an initial jump of the ambient pressure between 50 and 150 Pa, with observations of relative density differences $\Delta\rho/\rho$ from 0.001 to 0.017. The basic wave characteristics are typically: L_w ~ 3 to 10 km and a_w ~ 70 to 300 m.

Figure 17. Undular cloud pattern over Libourne (France) (Courtesy of Patrick Vialle)

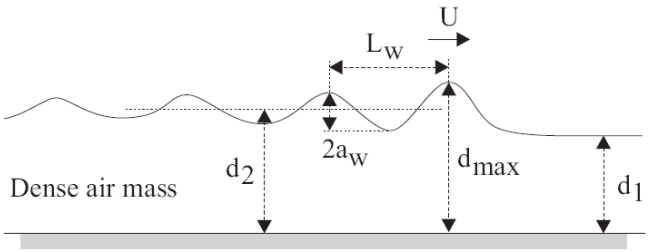

Figure 18. Sketch of an undular cloud formation

A number of researchers discussed the analogy between undular jumps and undular cloud formations (Clarke 1972, Christie 1992). There are clearly some important differences between a shallow water flow and a mass of dense air near the Earth's surface with three-dimensional variations of the air density. Neither the friction losses nor the thermodynamic processes can be neglected.

Nevertheless the field observations and numerical data provide some results that support the analogy (e.g. Clarke et al. 1981, Doviak and Ge 1984, Rottman and Simpson 1989). Figure 19 illustrates the velocity field during the passage of the first wave crest of an undular bore. The data are 2-minutes samples of the longitudinal and vertical wind velocities recorded with two independent techniques. In Figure 19, the undular cloud formation propagates from left to right. The data highlight the general streamline pattern as well as the velocity recirculation next to the ground beneath the wave crest. The data may be compared with Figures 13a and 14 in terms of the analogy with the undular tidal bore. The field data (Fig. 19) show further the large vertical velocity components. During another field observation, an instrumented aircraft flew in an undular bore, reporting very strong flow turbulence, with vertical accelerations of plus and minus 1.5 to 2×g (Lilly and Zipser 1972). At the about same time, a commercial Boeing 707 air cargo carrier

flew in the undular wave formation and "was [...] in real peril for a minute or so" (Lilly 1978).

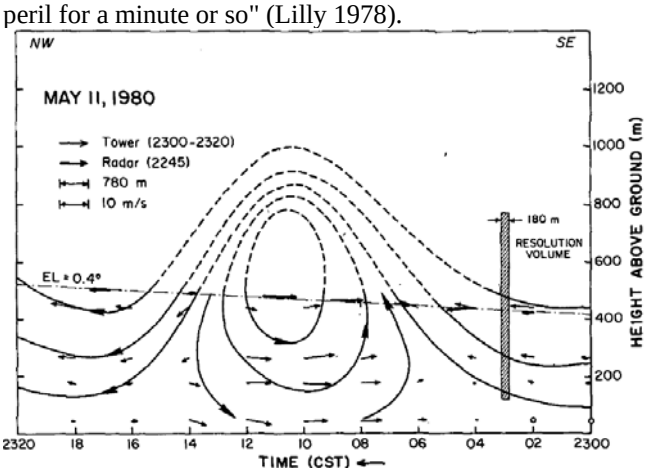

Figure 19. Wind d ata r ecords on 1 1 M ay 1980 i n Central Oklahoma during the passage of the firs t wave (Doviak and Ge 1984) - Data recor ded with a 444 m high instrumented tower and Dopppler radar

5. Conclusion

A tidal bore is a series of waves propagating upstream as the tidal flow turns to rising in an estuary. It forms during the spring tides when the tidal range exceeding 4 to 6 m is confined into a narrow funnelled estuary. When the difference in water elevations between the initial and new water levels is small to moderate, the tidal bore has an undular shape whereby the leading wave is followed by a train of well-developed free-surface undulations, also called whelps. The undular bore propagates upstream relatively slowly and the free-surface undulations have a smooth appearance; little wave breaking is observed but close to the banks or above sand banks. The meteorological equivalent is the undular bore cloud pattern that is known to cause some severe adverse impact on the air traffic.

An undular tidal bore takes place when the Froude number defined in the system of co-ordinates in translation with the bore front is less than 1.5 to 1.8 corresponding to a ratio of conjugate depths d_2/d_1 less than 1.7 to 2.1. The free-surface observations follow closely the momentum-specific energy diagram highlighting that the rate of energy dissipation is small. The free-surface undulations have a pattern somehow comparable to the sinusoidal and cnoidal wave functions, but neither the linear wave theory nor the Boussinesq equations can capture the fine details of the undular free-surface. The instantaneous velocity measurements show a rapid flow deceleration at all vertical elevations during the bore front propagation, and some large fluctuations of all velocity components are observed beneath the whelps. The large velocity fluctuations and Reynolds stresses recorded beneath the undulations imply the long-lasting impact of the undular bore passage. The velocity data suggest the production of energetic events and vorticity "clouds" beneath the bore front. This macro-turbulence is advected upstream behind the bore front. It is believed that the energetic turbulent events are generated by some transient secondary motion. The proposed mechanisms are consistent with some physical observations in the field as well as in laboratory, and some recent numerical simulations.

References

Andersen, V.M. (1978). "Undular Hydraulic Jump." *Jl of Hyd. Div.*, ASCE, Vol. 104, No. HY8, pp. 1185-1188. Discussion: Vol. 105, No. HY9, pp. 1208-1211.

Arrian (1976). *Arrian*. Harvard University Press, Cambridge, USA, translated by P.A. Brunt, 2 volumes.

Bazin, H. (1865). "Recherches Expérimentales sur la Propagation des Ondes." ('Experimental Research on Wave Propagation.') *Mémoires présentés par divers savants à l'Académie des Sciences*, Paris, France, Vol. 19, pp. 495-644 (in French).

Ben Meftah, M., De Serio, F., Mossa, M., and Pollio, A. (2007). "Analysis of the Velocity Field in a Large Rectangular Channel with Lateral Shockwave." *Env. Fluid Mech.*, Vol. 7, No. 6, pp. 519-536 (DOI: 10.1007/s10652-007-9034-7).

Benjamin, T.B., and Lighthill, M.J. (1954). "On Cnoidal Waves and Bores." Proc. Royal Soc. of London, Series A, Math. & Phys. Sc., Vol. 224, No. 1159, pp. 448-460.

Burk, S.D., and Haack, T. (2000). "The Dynamics of Wave Couds Upwind of Coastal Orography." *Monthly Weather Review*, Vol. 128, pp. 1438-1455.

Chanson, H. (1999). *The Hydraulics of Open Channel Flows: An Introduction*" Edward Arnold, London, UK, 512 pages.

Chanson, H. (2005). "Physical Modelling of the Flow Field in an Undular Tidal Bore." *Jl of Hyd. Res.*, IAHR, Vol. 43, No. 3, pp. 234-244.

Chanson, H. (2009). *Applied Hydrodynamics: An Introduction to Ideal and Real Fluid Flows*. CRC Press/Balkema, Taylor & Francis Group, Leiden, The Netherlands, 470 pages.

Chanson, H. (2010). "Unsteady Turbulence in Tidal Bores: Effects of Bed Roughness." *Journal of Waterway, Port, Coastal, and Ocean Engineering*, ASCE, Vol. 136, No. 5, pp. 247-256 (DOI: 10.1061/(ASCE)WW.1943-5460.0000048).

Chanson, H. (2011). "Undular Tidal Bores: Basic Theory and Free-surface Characteristics." *Journal of Hydraulic Engineering*, ASCE, Vol. 137 (**In Print**).

Chanson, H., and Montes, J.S. (1995). "Characteristics of Undular Hydraulic Jumps. Experimental Apparatus and Flow Patterns." *Journal of Hydraulic Engineering*, ASCE, Vol. 121, No. 2, pp. 129-144.

Chanson, H., and Tan, K.K. (2011). "Turbulent Mixing of Particles under Tidal Bores: an Experimental Analysis." *Journal of Hydraulic Research*, IAHR, Vol. 49 (**In Print**).

Christie, D.R. (1992). "The Morning Glory of the Gulf of Carpentaria: a Paradigm for Non-Linear Waves in the Lower Atmopshere." *Australian Met. Mag.*, Vol. 41, pp. 21-60.

Clarke, R.H. (1972). "The Morning Glory: an Atmospheric Hydraulic Jump." *J. Appl. Meteorology*, Vol. 11, pp. 304-311.

Clarke, R.H., Smith, R.K., and Reid, D.G. (1981). "The Morning Glory of the Gulf of Carpentaria – an Atmospheric Undular Bore." *Monthly Weather Rev.*, Vol. 109, No. 8, pp. 1726-1750.

Davis, R.E., and Acrivos, A. (1967). "Solitary Internal Waves in Deep Water." *Jl Fluid Mech.*, Vol. 29, Part 3, pp. 593-607.

Doviak, R.J., and Ge, R.S. (1984). "An Atmospheric Solitary Gust Observed with a Doppler Radar, a Tall Tower and a Surface Network." *Jl of Atmospheric Science*, Vol. 41, No. 17, pp. 2559-2573.

Dyer, K.R. (1997). *Estuaries. A Physical Introduction*. John Wiley, New York, USA, 2nd edition, 195 pages.

Favre, H. (1935). *Etude Théorique et Expérimentale des Ondes de Translation dans les Canaux Découverts*. ('Theoretical and Experimental Study of Travelling Surges in Open Channels.') Dunod, Paris, France (in French).

Furuyama, S., and Chanson, H. (2008). "A Numerical Study of Open Channel Flow Hydrodynamics and Turbulence of the Tidal Bore and Dam-Break Flows." *Report No. CH66/08*, Div. of Civil Engineering, The University of Queensland, Brisbane, Australia, May, 88 pages

Henderson, F.M. (1966). *Open Channel Flow*. MacMillan Company, New York, USA.

Hornung, H.G., Willert, C., and Turner, S. (1995). "The Flow Field Downstream of a Hydraulic Jump." *Jl of Fluid Mech.*, Vol. 287, pp. 299-316.

Koch, C., and Chanson, H. (2008). "Turbulent Mixing beneath an Undular Bore Front." *Journal of Coastal Research*, Vol. 24, No. 4, pp. 999-1007 (DOI: 10.2112/06-0688.1).

Koch, C., and Chanson, H. (2009). "Turbulence Measurements in Positive Surges and Bores." *Journal of Hydraulic Research*, IAHR, Vol. 47, No. 1, pp. 29-40 (DOI: 10.3826/jhr.2009.2954).

Lemoine, R. (1948). "Sur les Ondes Positives de Translation dans les Canaux et sur le Ressaut Ondulé de Faible Amplitude." ('On the Positive Surges in Channels and on the Undular Jumps of Low Wave Height.') *Jl La Houille Blanche*, Mar-Apr., pp. 183-185 (in French).

Lewis, A.W. (1972). "Field Studies of a Tidal Bore in the River Dee." *M.Sc. thesis*, Marine Science Laboratories, University College of North Wales, Bangor, UK.

Liggett, J.A. (1994). *Fluid Mechanics*. McGraw-Hill, New York, USA.

Lighthill, J. (1978). *Waves in Fluids*. Cambridge University Press, Cambridge, UK, 504 pages.

Lilly, D.K. (1978). "A Severe Downslope Windstorm and Aircraft Turbulence Event induced by a Mountain Wave." *Jl of Atmosph. Sc.*, Vol. 35, pp. 59-77.

Lilly, D.K., and Zipser, E.J. (1972). "The Front Range Windstorm of 11 January 1972. A Meteorological Narrative." *Weatherwise*, Vol. 25, No. 2, April, pp. 56-63.

Lubin, P., Glockner, S., and Chanson, H. (2010). "Numerical Simulation of a Weak Breaking Tidal Bore." *Mechanics Research Communications*, Vol. 37, No. 1, pp. 119-121 (DOI: 10.1016/j.mechrescom.2009.09.008).

Macdonald, R.G., Alexander, J., Bacon, J.C., and Cooker, M.J. (2009). "Flow Patterns, Sedimentation and Deposit Architecture under a Hydraulic Jump on a Non-Eroding Bed: Defining Hydraulic Jump Unit Bars." *Sedimentology*, Vol. 56, pp. 1346-1367 (DOI: 10.1111/j.1365-3091.2008.01037.x).

Montes, J.S. (1986). "A Study of the Undular Jump Profile." *Proc. 9th Australasian Fluid Mechanics Conference AFMC*, Auckland, New Zealand, pp. 148-151.

Montes, J.S. (1998). *Hydraulics of Open Channel Flow*. ASCE Press, New-York, USA, 697 pages.

Navarre, P. (1995). "Aspects Physiques du Caractère Ondulatoire du Macaret en Dordogne." ('Physical Features of the Undulations of the Dordogne River Tidal Bore.') *D.E.A. thesis*, Univ. of Bordeaux, France, 72 pages (in French).

Parker, G. (1996). "Some speculations on the relation between Channel Morphology and Channel Scale Flow Structures." in *Coherent Flow structures in Open Channels*, John Wiley, Chichester, UK, P.J. Ashworth, S.J. Bennett, J.L. Best and S.J. McLelland Ed., pp. 423-458.

Pond, S., and Pickard, G.L. (1983). *Introductory Dynamical Oceanography*. Butterworth Heinemann, Oxford, UK, 2nd edition, 329 pages.

Ponsy, J., and Carbonnell, M. (1966). "Etude Photogrammétrique d'Intumescences dans le Canal de l'Usine d'Oraison (Basses-Alpes)." ('Photogrammetric

Study of Positive Surges in the Oraison Powerplant Canal.') *Jl Soc. Française de Photogram.*, Vol. 22, pp. 18-28 (in French).

Quintus Curcius (1984). *The History of Alexander*. Penguin, New York, USA, translated by J. Yardley, 332 pages.

Rayleigh, Lord (1908). "Note on Tidal Bores." *Proc. Royal Soc. of London*, Series A containing Papers of a Mathematical and Physical Character, Vol. 81, No. 541, pp. 448-449.

Rottman, J.W., and Simpson, J.E. (1989). "The Formation of Internal Bores in the Atmosphere: a Laboratory Model." *Q. J. R. Meteorol. Soc.*, Vol. 115, pp. 941-963.

Rouse, H. (1938). *Fluid Mechanics for Hydraulic Engineers*. McGraw-Hill Publ., New York, USA (also Dover Publ., New York, USA, 1961, 422 pages).

Rulifson, R.A., and Tull, K.A. (1999). "Striped Bass Spawning in a Tidal Bore River: the Shubenacadie Estuary, Atlantic Canada." *Trans. American Fisheries Soc.*, Vol. 128, pp. 613-624.

Treske, A. (1994). "Undular Bores (Favre-Waves) in Open Channels - Experimental Studies." *Jl of Hyd. Res.*, IAHR, Vol. 32, No. 3, pp. 355-370. Discussion : Vol. 33, No. 3, pp. 274-278.

Wolanski, E., Williams, D., Spagnola, S., and Chanson, H. (2004). "Undular Tidal Bore Dynamics in the Daly Estuary, Northern Australia." *Estuarine, Coastal and Shelf Science*, Vol. 60, No. 4, pp. 629-636.

Wood, I.R., and Simpson, J.E. (1984). "Jumps in Layered Miscible Fluids." *Jl Fluid Mech.*, Vol 140, pp. 329-342.